Supporting Information

For

A Multifunctional Nanosensor Based on Silica Nanoparticles and Biological Applications in Living Cell

Wenyu Wu,[a] Zhihong Sun,[b] Ye Zhang,[a] Jun Xu,[a] Huisheng Yu,[a] Xiao Liu,[a]

Qin Wang,[b] Weisheng Liu,[a] and Yu Tang[a]*

[a]Key Laboratory of Nonferrous Metal Chemistry and Resources Utilization of Gansu Province, State Key Laboratory of Applied Organic Chemistry, College of Chemistry and Chemical Engineering, Lanzhou University, Lanzhou, P. R. China

[b]Institute of Cancer Biology and Drug Screening, School of Life Science, Lanzhou University, Lanzhou, P. R. China.

General experimental procedures

Characterization of RFSNP

Fluorescence study

Biological study

References of S.I.

General experimental procedures

Instrumentation

Transmission electron microscopy (TEM) images were taken on a Tecnai-G2-F30 (300 kV). Dynamic light scattering (DLS) measurements were performed by a BI-200SM from Brookhaven Corporation (America). Hydrodynamic particle diameters were obtained from cumulant fits of the autocorrelation functions at 90 scattering angle. Fourier transform infrared (FT-IR) spectra were conducted within the 4000-400 cm^{-1} wavenumber range using a Nicolet 360 FT-IR spectrometer with the KBr pellet technique. Thermogravimetric (TG) analyses were performed on a Perkin-Elmer thermal analyzer up to 800 °C at a heating rate of 10 °C/min under nitrogen atmosphere. Powder X-ray diffraction patterns (PXRD) were determined with Rigaku-Dmax 2400 diffractometer using Cu Kα radiation over the 2θ range of 10-80º. X-Ray photoelectron spectroscopy (XPS) measurements were carried out on a PHI-5702 multi-functional spectrometer using Al Kα radiation. ^{1}H NMR spectra were recorded on a Bruker 400 MHz spectrometer. Chemical shifts (δ) are given in parts per million (ppm), and coupling constants (J) are given in Hertz (Hz). Mass spectra (EI) were obtained on HP 5988A GC-MS spectrometers. The UV-vis absorption spectra were recorded on a Perkin Elmer Lambda 950 spectrophotometer. Steady state luminescence spectra were measured on a Hitachi F-4500 fluorescence spectrophotometer. Quantum yields were determined by an absolute method using an integrating sphere on Edinburgh Instrument FLS920. The overall quantum yields Φ measured were determined by an absolute method using an integrating sphere (150 mm diameter, $BaSO_4$ coating) with three measurements carried out for each sample.

Reagent

N-(2-Hydroxyethyl)piperazine-N'-2-ethanesulfonic acid (HEPES) was purchased from Acros Organic Company. All other chemicals were purchased from Sigma-Aldrich and were used as received. Deionized water was used to prepare all aqueous solutions. Stock solutions of perchlorate salts of the respective ions (Li^+, Na^+, K^+, Cs^+, Mg^{2+}, Ca^{2+}, Fe^{2+}, Fe^{3+}, Co^{2+}, Ni^{2+}, Cu^{2+}, Zn^{2+}, Cd^{2+}, Pb^{2+}, Ba^{2+}, Sr^{2+}, Cr^{3+}, and Hg^{2+}) were prepared with deionized water. The RFSNP solution (1mM) was prepared in H_2O/ethanol (50 mM HEPES buffer, pH 7.2, 1:1, v/v) medium. The complex RFSNP-Hg^{2+} solutions were prepared by adding the Hg^{2+} stock solution through a micro-pipette to 2 mL of a RFSNP solution (10 or 20 μM). The anions used in fluorescence experiment were all tetrabutylammonium (TBA) salts. The emission spectra of the fluorescent nanoparticle suspension with different concentrations of Hg^{2+} and $H_2PO_4^-$ anion solutions [or other anions S^{2-}, SCN^-, CN^-, $H_2PO_4^-$, N_3^-, HSO_4^-, NO_3^-, AcO^-, I^-, F^-, BF_4^-, ClO_4^-, HS^-, HSO_3^-, PF_6^-, Br^-.] were measured. All measurements were repeated three times, and the general average was obtained. For details of all experimental procedures, characterization data of the nanosensor, and other fluorescence data, see the Supporting Information.

Calculations for the binding constants using spectrophotometric titration Data

The association constant and stoichiometry for the formation of the were evaluated using the Benesi-Hildebrand (B-H) plot [Eq. (1)].[1]

$$1/(F-F_0)= 1/K(F_{max}-F_0)[M^{n+}]+ 1/(F_{max}-F_0) \quad (1)$$

Binding stoichiometry for the complex formation is confirmed from Job's plot. In the case of evaluation of the binding constant from the results of fluorescence titration, a modified B-H equation [Eq. (1)] is used, where F_0, F_{max}, and F represent the emission intensity of RFSNP, the maximum emission intensity observed in the presence of Hg^{2+} at 578 nm, and intensity at a certain concentration of the metal ion, respectively. K is the association constant (M^{-1}) and was

determined from the slope of the linear plot, and [M^{n+}] is the concentration of the Hg^{2+} ion added during titration studies.

Cell line and culture conditions

The HEK 293T and HeLa cell lines were provided by the Institute of Cancer Biology and Drug Screening, Lanzhou University. The cells were grown in DMEM medium (Sigma) supplemented with 10% fetal bovine serum (Hyclone), 2 mM l-glutamine, 100 units mL^{-1} penicillin and 100 mg mL^{-1} streptomycin and incubated at 37°C in a humidified atmosphere of 5% CO_2 and 95% air.

Determination of cell viability

Cell viability was determined by 3-(4,5-dimethylthiazol-2-yl)-2,5-diphenyl-tetra-zolium bromide (MTT, Amresco 0793) assays as we have previously described.[2] HEK 293T and HeLa cells (1×10^4 cells/well) were placed in a flat-bottom 96-well plate (Costar) in 100 μL culture medium and incubated in 5% CO_2 at 37 °C. After overnight incubation, the cells were treated with RFSNP concentrations of 5, 10, 20, 30, 50, 100 μM. After incubating the cells and nanosensor for 24 h, the MTT reagent (5 mg mL^{-1}) was then added to each well (10 μL/well, 0.5 mg mL^{-1}) and incubated 4 h. The water-insoluble formazan crystal was dissolved by the addition of 100 μL of DMSO to each well. The optical density of each well was measured with a using a Perkin Elmer $VICTOR_3$ 1420 Multilabel Plate Reader at 490 nm. The relative cell viability (mean% ± SD, n = 3) was expressed as Abs compound/Abs control, where Abs control was obtained in the absence of the compounds.

The MTT assay including a positive control as well as a negative was carried out. NH_2-functionalized silica nanoparticle was used as positive control. Meanwhile, the negative control is the rhodamine derivative RDd, which has larger cell toxicity than the nanosensor. The cytotoxicity decreased significantly after covalent grafting of the organic ligands onto the nanoparticle.

Crystal Violet staining

HeLa cell line was cultured in DMEM (Hycone), containing 10% FBS (Gibco), in 6-well plate (Costar) and treated with 5 μM, 10 μM, 20 μM, 30 μM, 50 μM, 100 μM RFSNP for 24 h. After the culture medium was pumped out by a vacuum pump, cells were washed twice with PBS and then add appropriate amount of 95% ethanol to fixate the cells for 30 min at room temperature.

Discard the ethanol and add appropriate amount of crystal violet solution and keep it for 30 min at room temperature. Recycle the crystal violet solution and wash the cells with PBS for 4 times to decolor the background. Then, pump the water by a vacuum pump. The cells morphological features were examined by Nikon Ti-U Fluorescent Inverted Microscope and the photos were taken with a digital camera (COOPLIX P5100, Nikon).

Test of intracellular ion concentrations and pH change

Cells at 80% confluence were treated overnight with RFSNP at the indicated concentrations (20 μM). The cell culture medium was removed, as well as washed twice with deionized water speedily before collection in ep tube. Thereupon the cells were treated with ultrasound for 90 seconds by Ultrasonic instrument. Then, we measure the pH value and concentration changes of calcium and mercury ions after the addition of mercury. Flame atomic absorption spectroscopy has been used to determine the concentration of Ca^{2+} and Hg^{2+} ions.

Cell fluorescence

HeLa cells (5×10^4 cells/well) were seeded in a flat-bottom 6-well plate (Costar) with glass coverslips in 2 ml culture medium and incubated in 5% CO_2 at 37 °C. After overnight incubation，the cells were treated with 20 μM RFSNP for 12 h and washed three times with PBS before incubating with 20 μM $Hg(NO_3)_2$ for another 0.5 h, finally 100 μM Na_2S was

added as the fluorescence quenches agent. Then the fluorescence imaging of cell membrane was observed under 490 nm (Zeiss Leica DM 4000B microscope, 40X objective lens). The HeLa cells only incubated with 20 μM RFSNP for 12 h at 37 ºC under 5% CO_2 was as a control.

1. Synthesis of the functionalized optical material

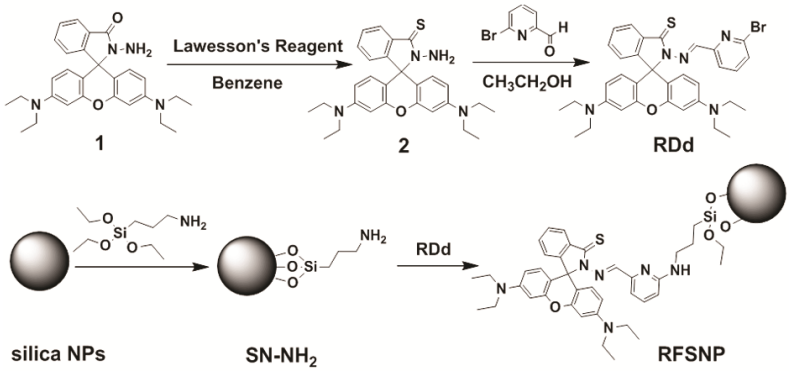

Fig. S1 Synthesis procedure for the functionalized optical material RFSNP

Synthesis of the rhodamine derivative RDd

Rhodamine B hydrazide was synthesized according to previous literature reports.[3] Thiooxorhodamine B hydrazone was synthesized according to the literature method and identified by NMR and mass data.[4] Thiooxorhodamine B hydrazide (1.50 mmol, 0.71 g) and 6-bromopicolinaldehyde (1.60 mmol, 0.30 g) were mixed in 30 mL of boiling ethanol with addition of 3 drops of acetic acid as catalyst. After 8 h of stirring, white precipitates of RDd obtained were filtered off, washed with methanol, and dried under vacuum. Yield: 0.52 g, 54.1%.

^{1}H NMR ($CDCl_3$, 400 MHz) δ (ppm): 8.55 (s, 1H), 8.16 (br, 1H), 8.06 (d, J = 7.6 Hz, 1H), 7.50 (t, J = 7.2 Hz, 1H), 7.44 (m, 3H), 7.14 (d, J = 7.2 Hz, 1H), 6.75 (s, 2H), 6.34 (s, 4H), 3.32 (q, J = 7.0 Hz, 8H),1.15 (t, J = 7.0 Hz, 12H). Mass (ESI-MS): (m/z,%): 642.1 (M+H).

Preparation of NH_2-functionalized SiO_2 nanoparticles ($SN\text{-}NH_2$)

3-Aminopropyl triethoxysilane (APTES, 2 mL) was dissolved in anhydrous toluene (200 mL) and silica nanoparticles [5] (1 g) were added. The mixture was treated under ultrasonication for 30 min and stirred at 90 °C for 24 h. The product was separated by centrifugation at 12000 rpm for 10 min. The collected solid was washed several times with ethanol by repetitive dispersion and precipitation cycles to rinse away raw material.

Synthesis of the rhodamine-derivant functionalized optical nanoparticles RFSNP

As shown in Fig. S1, 1.0 g of $SN\text{-}NH_2$ was dispersed in 200 mL anhydrous toluene and under sonicate for 30 min. Then 0.5 g of the as-prepared RDd and 0.1 g Cs_2CO_3 was added and the mixture was refluxed for 24 h. The product was separated by centrifugation at 12000 rpm for 10 min. The collected solid was washed several times with dichloromethane and ethanol with repetitive dispersion/precipitation cycles to rinse away any excess 3-aminopropyl triethoxysilane and RDd, and then dried under vacuum.

Characterization of RFSNP

2. TEM and DLS image

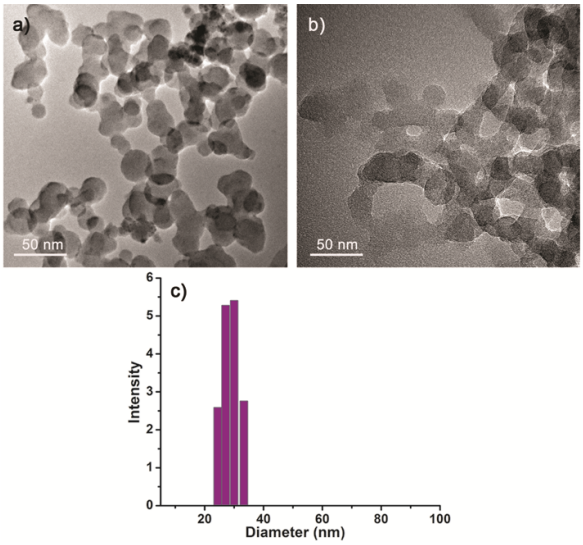

Fig. S2 TEM images of a) unmodified SN and b) modified optical nanohybrid RFSNP, where the scale bar = 50 nm. c) Particle size distribution of RFSNP (2 mg/L, suspended in aqueous medium), measured by DLS.

3. FT-IR spectroscopy

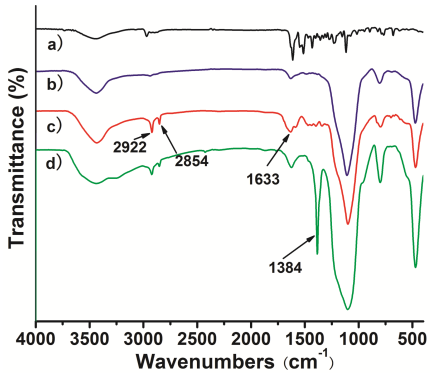

Fig. S3 FT-IR spectra of a) RDd, b) SN-NH_2, c) RFSNP and d) RFSNP-$Hg(NO_3)_2$.

4. Thermogravimetric and elemental analysis of SN-NH_2, RFSNP and RFSNP-Hg^{2+}

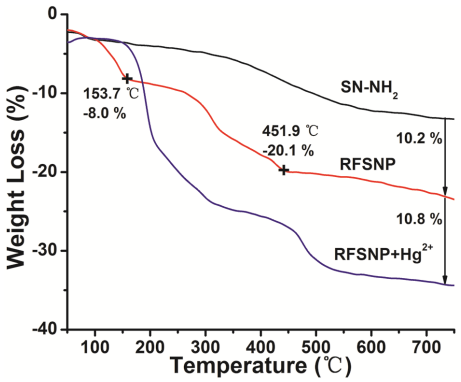

Fig. S4 Thermogravimetric analysis plot of SN-NH_2, RFSNP and RFSNP-Hg^{2+}, loss of physisorbed water completes at 154 °C, constant weight after 452 °C.

When the samples were heated from room temperature to 750 °C, after the initial weight loss of water molecules, the RFSNP began to lose organic block.[6] A major weight loss region between 153.7 and 451.9 °C of the organic ligand chemically bonded to the surface (12%). The content of mercury combined with the material was surveyed by ICP

(measured concentration: 21%, theoretical concentration: 25%) to rectify the actual rate of graft.

Table. S1 Elemental analysis data of RFSNP and RFSNP-Hg^{2+}.

	N [%]	C [%]	H [%]
RFSNP	1.72	9.03	1.85
RFSNP-Hg^{2+}	1.69	6.65	1.22

5. Powder X-ray diffraction (PXRD) patterns of RDd, SN-NH_2, and RFSNP

PXRD patterns of silica nanohybrids indicated that the parent silica support was completely amorphous. Grafting of the chromophores did not result in any changes in the patterns.

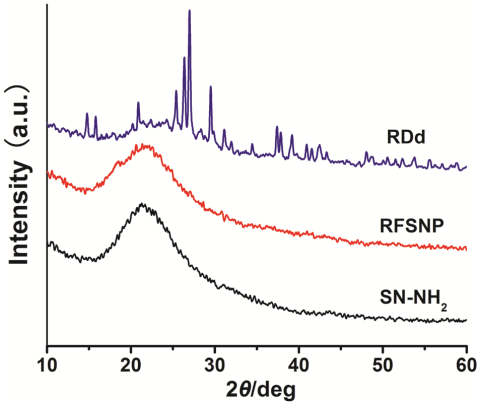

Fig. S5 Powder X-ray diffraction (PXRD) patterns of RDd, SN-NH_2, and RFSNP.

Fluorescence study

6. Visible color changes by naked eyes under UV irradiation and natural light.

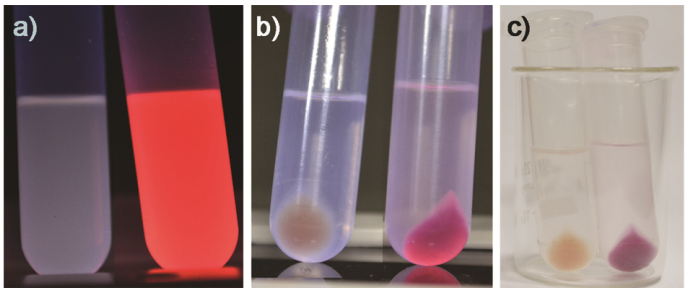

Fig. S6 Visible color changes before and after RFSNP binding with Hg^{2+} by naked eyes: a) Decentralized systems by ultrasonic in aqueous solution under UV irradiation. b) The systems after centrifugation under overlay of UV irradiation and natural light. c) After centrifugation in the natural light.

7. Fluorescence Job's plot and titration curve of RFSNP with Hg^{2+}

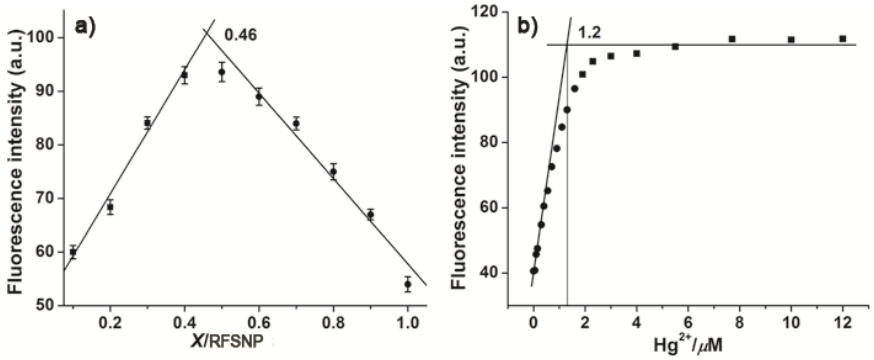

Fig. S7 a) Fluorescence Job' plot for RFSNP with Hg^{2+} in H_2O/ethanol (1:1, v/v). The total [RFSNP] + [Hg^{2+}] = 10.0 μM. b) Titration curve of RFSNP (10 μM/2.0 mL) in the presence of Hg^{2+} from 0.01 to 12.0 μM.

8. Fluorescence and UV-Vis titration spectra of RFSNP to different amounts of Hg^{2+}

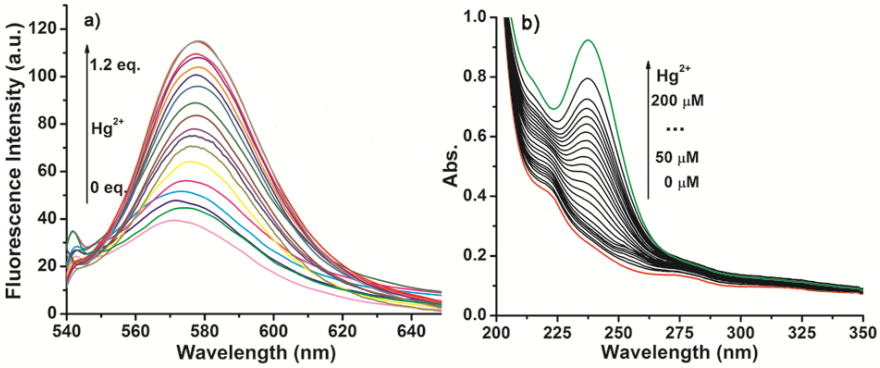

Fig. S8 a) Fluorescence and b) UV-Vis titration spectra of RFSNP (10 μM) in H_2O/ethanol (1:1, v/v) at pH 7.2 upon exposure to different amounts of Hg^{2+}. All spectral data were recorded at 3 min after the Hg^{2+} addition.

9. ^{1}H NMR spectra of RDd before and after the addition of different amounts of Hg^{2+} ions

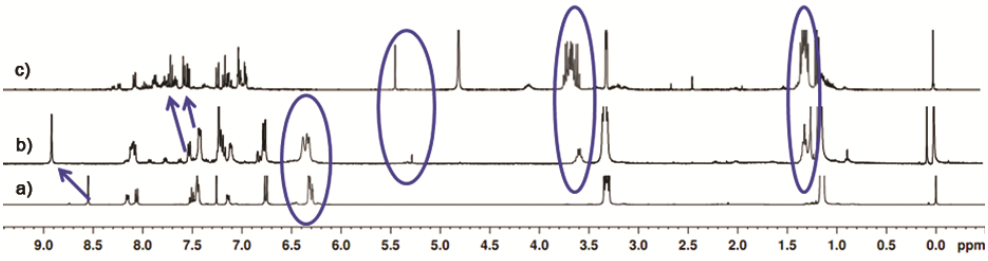

Fig. S9 Evolution of the ^{1}H NMR spectra of RDd in $CDCl_3$ upon addition of increasing amounts of Hg^{2+} (CD_3OD), from a) RDd only, b) 0.5 equiv. Hg^{2+} added, to c) 1 equiv. Hg^{2+} added.

Upon gradual addition of Hg^{2+} cations (0, 0.5, 1.0 equiv.) to a solution of RDd, the =C– proton upshifted by 0.4 ppm, clearly revealing one of the very binding sites. The two neonatal bands emerging around 3.65 and 1.30 ppm indicate that the Hg^{2+} complex with RDd prefers to exist in enol form, as shown in Scheme 1.

10. Fluorescence B-H linear fitting RFSNP-Hg^{2+} with $H_2PO_4^-$

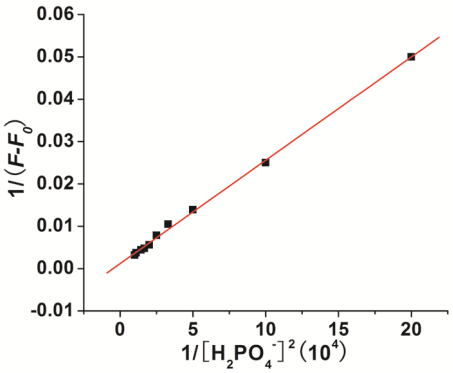

Fig. S10 Corresponding linear regression plot of $1/(F\text{-}F_0)$ vs. $1/[H_2PO_4^-]^2$ M^{-1}. $Y = 1.17\times10^{-3} + 2.44\times10^{-7}\ X$ (R^2 = 0.9983).

11. X-ray photoelectron spectroscopy of the molecular characterization on the RFSNP and RFSNP-$Hg(NO_3)_2$-NaH_2PO_4

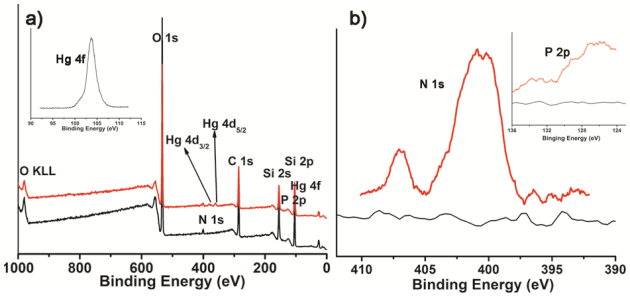

Fig. S11 a) Al Kα excited XPS spectra of the RFSNP nanohybrid before and after binding with $Hg(NO_3)_2$ and NaH_2PO_4. b) The N1s energy region for the RFSNP binding with Hg^{2+} and $H_2PO_4^-$ after basic washing, a grafted rhodamine molecule binding with the Hg^{2+} and $H_2PO_4^-$ ions, accounting for the higher binding energy shoulder. Insets are the high-resolution spectra of a) Hg 4f and b) P 2p.

12. Fluorescence responses of RFSNP-Hg^{2+} (20 μM) upon addition of various aions and titration curve of RFSNP-Hg^{2+} with S^{2-}

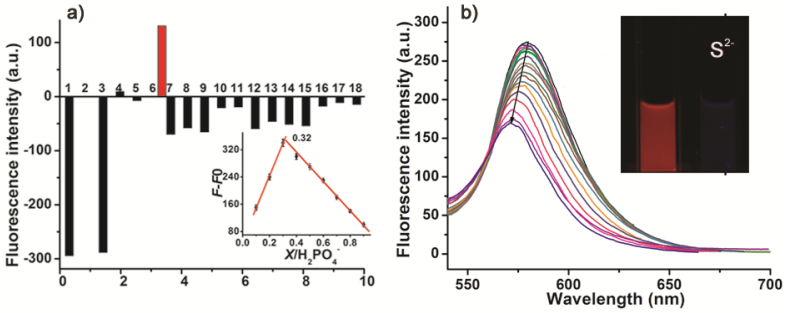

Fig. S12 a) Fluorescence responses of RFSNP-Hg^{2+} (20 μM) upon addition of various aions (0.1 mM). 1, RFSNP; 2, RFSNP-Hg^{2+}; 3, RFSNP-Hg^{2+}-S^{2-}; 4, SCN^-; 5, CN^-; 6, $H_2PO_4^-$; 7, N_3^-; 8, HSO_4^-; 9, NO_3^-; 10, AcO^-; 11, I^-; 12, F^-; 13, BF_4^-; 14, ClO_4^-; 15, HS^-; 16, HSO_3^-; 17, PF_6^-; 18, Br^-. b) Fluorescence titration curve of RFSNP-Hg^{2+} (20 μM/2.0 mL) in the presence of S^{2-} as an aqueous solution of Na_2S from 0 to 40.0 μM. Inset of a): Fluorescence Job's plot for RFSNP-Hg^{2+} with $H_2PO_4^-$. Total [RFSNP-Hg^{2+}] + [$H_2PO_4^-$] = 60 μM. Inset of b): Visible color changes before and after S^{2-} addition.

All spectral data were recorded at 10 min after the addition of different anions in H_2O/ethanol (1:1, v/v, pH 7.2), with an excitation at 523 nm.

13. Regeneration ability of RFSNP

The reusability of RFSNP was evaluated by repeated complexation–stripping cycles with the fluorescence spectra recorded after each step. This process could be repeated at least four times.

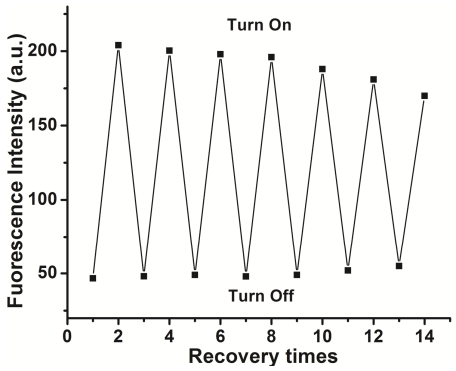

Fig. S13 Fluorescence responses of RFSNP (10 μM) by alternated adding Hg^{2+} (20 μM) in H_2O/ethanol (1:1, v/v, 20 mM HEPES, pH 7.2) system (Turn On) and 100 μM of S^{2-} (sodium salt) (Turn Off) over seven complex/stripping cycles. The strength of the above corresponds to the emission of RFSNP with Hg^{2+} solutions (λ_{ex} = 523 nm, λ_{em} = 578 nm).

Biological study

14. Determination of cell viability

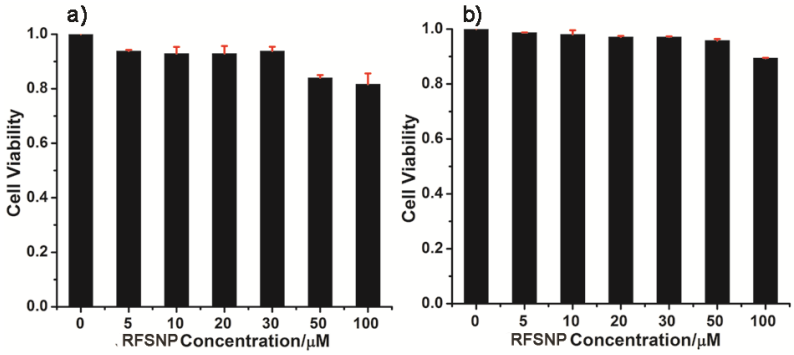

Fig. S14 MTT assay for the viability of HEK 293T a) and HeLa cell b) treated with various concentrations of RFSNP for 24 h. Error bars represent the standard deviations of 4 trials.

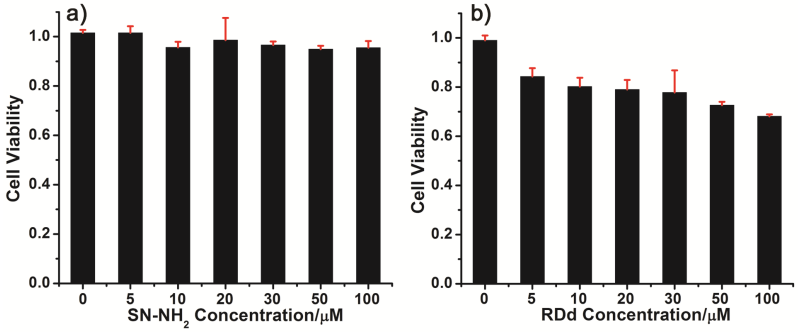

Fig. S15 The MTT assay positive control a) and negative control b). The positive control is used NH_2-functionalized

silica nanoparticle, and the negative control is rhodamine derivative RDd.

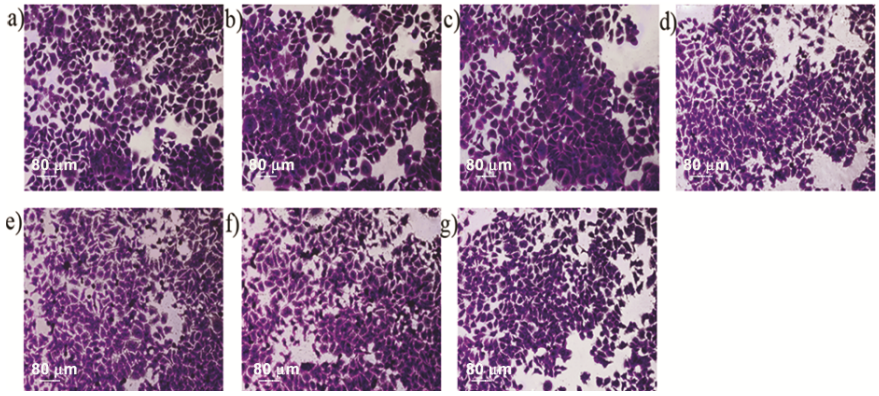

Fig. S16 Crystal violet stain. Bright–field measurements after treatment with RFSNP a), b), c), d), e), f), g): Control, 5 μM, 10 μM, 20 μM, 30 μM, 50 μM, 100 μM. (Nikon Ti–U Fluorescent Inverted Microscope, 10×objective lens).

15. Intracellular changes in pH value and concentration of Ca^{2+} and Hg^{2+} ions

Table. S2 Changes of Ca^{2+} and Hg^{2+} concentrations and pH value after the addition of RFSNP and Hg^{2+}. Cells-RFSNP-Hg^{2+} were treated overnight with RFSNP (20 μM), and then incubated with Hg^{2+} for 30 min.

cell sample	Ca^{2+}/μM	Hg^{2+}/μM	pH values
blank	80.7	—	7.19
Cells-RFSNP-Hg^{2+}	552	5.89	6.78

16. Cell imaging study

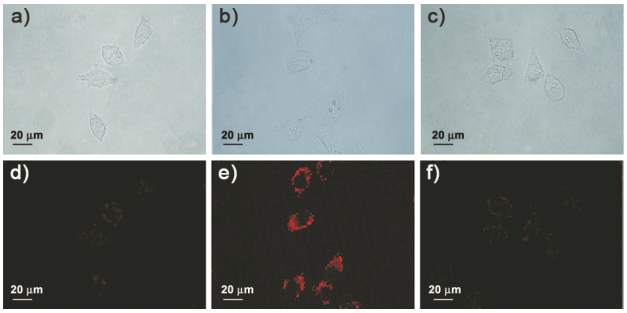

Fig. S17 Fluorescence microscopy images of HeLa cells a), d) HeLa cells after incubation with RFSNP 15 μM 12 h. b), e) HeLa cells after incubation with RFSNP 15 μM 12 h, then added Hg^{2+} 15 μM for 0.5 h at 37 °C, emission measured at 490 nm. c), f) HeLa cells after incubation with RFSNP 15 μM 12 h and Hg^{2+} 15 μM 0.5 h, then added Na_2S 100 μM for 10 min. (a, b and c) A bright-field transmission image of HeLa cells, (d, e, f) fluorescence images of HeLa cells (Zeiss Leica DM 4000B microscope, 40X objective lens).

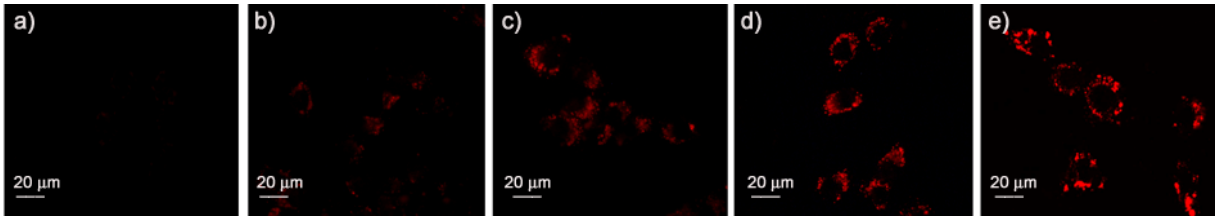

Fig. S18 Fluorescence microscopy images of Hg^{2+}-treated HeLa cells. The cells were supplemented with 20.0 μM RFSNP for 12.0 h in the growth media at 37 °C, followed by staining with different concentrations of $Hg(NO_3)_2$ (0.0 μM; 5.0 μM; 10.0 Mm; 15.0 μM; 20.0 μM;) for 1.0 h at 37 °C.

References of S.I.

[1] (a) Y. Shiraishi, S. Sumiya, Y. Kohno, T. J. Hirai, *Org. Chem*., 2008, **73**, 8571; (b) S. Sukdeb, M. Prasenjit, R.G. Upendar, E. Suresh, C. Arindam, B. Mithu, K. G. Sudip, D. Amitava, *Inorg. Chem*., 2012, **51**, 336; (c) Y. Hong, Z. G Zhou, K. W. Huang, M. X. Yu, F. Y. Li, T. Yi, C. H. Huang, *Org. Lett*., 2007, **9**, 4729; (d) Y. Xiang, A. J. Tong, P. Y. Jin, Y. Ju, *Org. Lett*., 2006, **8**, 2863.

[2] W. D. Wang, X. M. Xu, Y. Chen, P. Jiang, C. Z. Dong, Q. Wang, *Archives of Pharmacal Research*, 2009, **32**, 1727.

[3] V. Dujols, F. Ford, A. W. Czarnik, *J. Am. Chem. Soc*., 1997, **119**, 7386.

[4] H. Zheng, Z. H. Qian, L. Xu, F. F.Yuan, L. D. Lan, J. G. Xu, *Org. Lett*., 2006, **8**, 859.

[5] W. Stöber, A. Fink and E. Bohn, *J. Colloid Interface Sci*., 1968, **26**, 62.

[6] (a) M. H. Lee, S. J. Lee, J. H. Jung, H. Lima, J. S. Kim, *Tetrahedron*, 2007, **63**, 12087; (b) W. Huang, D.Y. Wu, G. H. Wua, Z. Q. Wang, *Dalton Trans*., 2012, **41**, 2620.